

IN-SITU CHARACTERIZATION OF AUSTENITE TO MARTENSITE DECOMPOSITION IN 9CR-1MO-V STEEL WELDS

M. L. Santella, S. S. Babu, R. W. Swindeman, and E. D. Specht

Oak Ridge National Laboratory, Oak Ridge, TN 37831

Abstract

The austenite decomposition behavior of a 9Cr-1Mo-V base metal and weld metal was characterized using dilatometry and in-situ x-ray diffraction. Experimental measurements were made as samples were austenitized at 1040°C, cooled to room temperature at 6°C/min, tempered at 740°C, and cooled a second time to room temperature. The data show that transformation of austenite to martensite was completed in the base metal during cooling from 1040°C. In contrast, the initial cooling from 1040°C did not completely transform austenite in the weld metal to martensite. Austenite retained in the weld metal was stable during the tempering treatment and only transformed to martensite during the final cooling stage. The diffraction data also showed that the austenite lattice parameter in the weld metal decreased during the tempering treatment. This observation was consistent with the retained austenite having a higher M_s than it did during the initial cooling. Computational thermodynamics modeling was used to predict that the elements, C, Cr, Mn and Ni, that influence transformation temperatures in this alloy strongly partition to interdendritic regions during solidification. The stability of retained austenite in the weld metal during the thermal cycle and its transformation behavior were attributed to the effects of microsegregation. After the final cooling from the tempering treatment the weld metal will contain a small amount of untempered martensite.

Introduction

In the early 1980's, tubing of 9Cr-1Mo-V (P91) steel was introduced into the superheaters of power boilers [1]. Because P91 steel is a air-hardenable martensitic high-strength alloy [2], the specifications of preheating and post weld heat treating conditions are critically important [3,4]. One aspect of this issue is the handling of welded components between the time that welding is completed and post weld heat treatment begins. Weldments that are cooled to room temperature before post weld heat treatment will transform more completely to martensite than those that are maintained at or above minimum preheat temperatures (200-300°C) prior to post weld heat treatment (740-780°C). Consequently, weldments that are cooled to room temperature are less likely to contain untempered martensite after post weld heat treatment. However, maintaining preheat temperature before post weld heat treatment is essential for minimizing the probability of hydrogen cracking in weld heat-affected zones. Adding to the complexities of post weld heat treatment are the inherent differences between base metal and weld metal microstructures. The base metal will generally be in the wrought condition and it may contain only minimal remnants of as-cast solidification microstructure such as compositional banding or primary carbides. In contrast, the weld metal microstructure will be characterized by distinct solute segregation resulting from the solidification process. The differences between the base metal and weld metal microstructures mean that their responses to the same post weld heat treatment may not be identical.

This paper describes the austenite decomposition behavior of a submerged arc weld deposit made in 50-mm-thick P91 plate and post weld heat treated for 8 hours at 774°C, and compares

it to the transformation behavior of a normalized and tempered P91 plate. The transformation behaviors were determined from specimen dilations measured during controlled heating and cooling, and from in-situ time-resolved diffraction measurements conducted at a synchrotron. Calculations from computational thermodynamics were used to help rationalize the observed behaviors.

Experimental

Materials and Welding Procedure

The chemical compositions of the submerged arc weld deposit and the plate material used for this work are given in Table I. The submerged arc weld was made using Thermanit MTS3 welding filler metal and Marathon 543 flux (Böhler Thyssen). A total of 44 weld beads was used to complete the 50-mm-thick weldment. The weldment was given a post weld heat treatment of 8 hours at 774°C before being supplied for testing and analysis. Specimens from normalized-and-tempered plate identified as heat 30383 were used to establish baseline transformation behavior for P91 plate. The microstructures in both the weld deposit and the plate consist of tempered martensite and a number of precipitate phases including $M_{23}C_6$, Fe_3C , and Nb and V carbonitrides [5,6].

Table I. Alloy chemical compositions

Analyzed composition, wt%										
ID/heat	C	Mn	Si	Cr	Mo	Ni	Nb	V	N	Al
Weld	0.099	0.61	0.17	9.33	0.97	0.80	0.043	0.23	0.051	0.022
30383	0.083	0.46	0.41	8.46	1.02	0.09	0.072	0.198	0.051	0.002

Dilatometry

A Gleeble™ 3500 thermomechanical simulator was used to determine the M_S temperatures. The Gleeble specimens were 6.35-mm-diameter-x-108-mm-long rods. In the weld deposit, the rods were cut transverse to the welding direction from near the weld surface. The width of the weld at this location was about 45 mm, insuring that the section of the specimen that was actually heated was entirely within the weld deposit. Variations of the specimen diameters during heating and cooling were measured with an LVDT strain gauge configured to detect the dilations. The strain gauge was attached at the same location along the specimen length as the thermocouple. The specimens were heated either in vacuum (0.1-1 Pa) or argon atmosphere to minimize oxidation during testing. Transformation temperatures were determined by curve fitting procedures at points of significant discontinuity on dilation-versus-temperature data plots [7]. The apparent variations of specimen diameters during isothermal tempering and austenitizing segments were ignored because of the difficulties of unambiguously associating them with phase transformations in the specimens. [8]. Small inflections found at the end of the thermal cycles were associated with termination of the heating program and these were also ignored. A thermal cycle representative of those used for the austenitizing and tempering treatments is shown in Fig.1. The heating rate for austenitizing at 1040°C of about 33°C/s, and the 2 min isothermal hold at 1040°C were chosen as experimental conveniences to reduce the probability of thermocouple deterioration during the thermal cycles. Combined with the 6°C/min cooling rate these conditions produced total austenitizing times of about 38 min for the weld deposit and about 30 min for the plate. The estimated A_3 's were 825°C for the weld deposit and 859°C for the plate.

Time-resolved X-ray Diffraction

Specimens with dimensions of 4.8 mm x 1 mm x 112 mm were cut from the plate and from the top of the weld for the diffraction measurements. The specimens were subjected to the same

nominal heat treatment shown in Fig. 1 while arranged for x-ray diffraction in a synchrotron beam line. Specimen temperatures were controlled by AC resistive heating to $\pm 0.2^\circ\text{C}$. A shroud of flowing helium was used to minimize oxidation. X-rays with wavelength $\lambda = 0.041328$ nm were provided by the UNICAT X-33 undulator beamline at the Advanced Photon Source. At this energy, x-rays penetrate about 0.16 mm into steel, so diffraction from the near-surface region is relatively weak. The x-rays were incident at a 7.5° glancing angle. A 2D image of the diffracted x-rays was recorded every 8 sec. Diffracted x-rays were filtered through 3-mm-thick Al to remove fluorescence and recorded using a Princeton Instruments model SCX-1242E CCD camera with 1152 x 1242 pixels, a 0.0225 mm x 0.0225 mm pixel size and 16-bit resolution. The detector was placed 97 mm from the sample, measuring plane spacings of $0.10 \text{ nm} < d < 0.25 \text{ nm}$. The detector was calibrated using Si powder (NIST SRM 640b, $d = 0.54311946$ nm). The 2-D diffraction rings were summed to obtain traditional intensity-versus- 2θ plots. During measurement, weak diffraction appeared from $(\text{Fe,Cr})_2\text{O}_3$, which formed from residual O_2 in the He atmosphere.

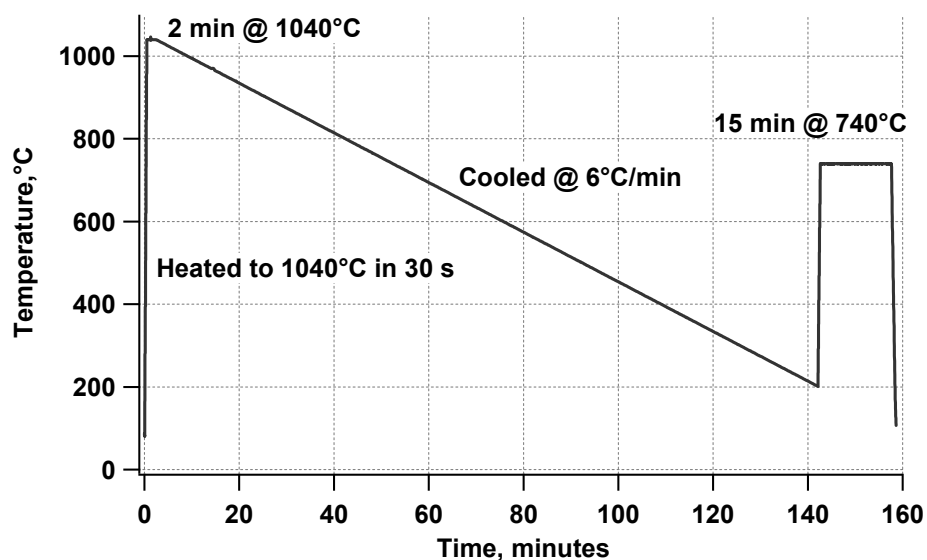


Figure 1. Thermal cycle used for heat treatments.

Results and Discussions

Dilatometry

The specimen dilation results for the base metal and the weld metal are shown respectively in Fig. 2(a) & (b). The M_S for base metal was 393°C , and the martensite reaction appeared to be completed prior to the tempering portion of the treatment because no other phase transformation was detected. In contrast, the primary M_S for the weld deposit was 350°C , and a secondary M_{S2} was detected near 400°C . These results indicate that the austenitized weld deposit may not have transformed completely with initial cooling, and that austenite was present in the microstructure after the tempering treatment.

The M_S temperatures for both the base metal and the weld metal agree well with published expressions for the prediction of this transformation start temperature [9,10]. The predicted and measured M_S 's for base metal are 383°C and 393°C ; those for the weld metal are 348°C and 350°C . The behavior of the base metal is also consistent with analysis indicating that $M_F = M_S - (180-200^\circ\text{C})$ [9]. Based on this relationship, the martensite transformation in the base metal should be completed after cooling to about $190-210^\circ\text{C}$. An M_F in this range is consistent with the dilation measurements shown in Fig. 2(a). These data show that cooling to room temperature is enough to completely transform austenite to martensite, or at least to a level

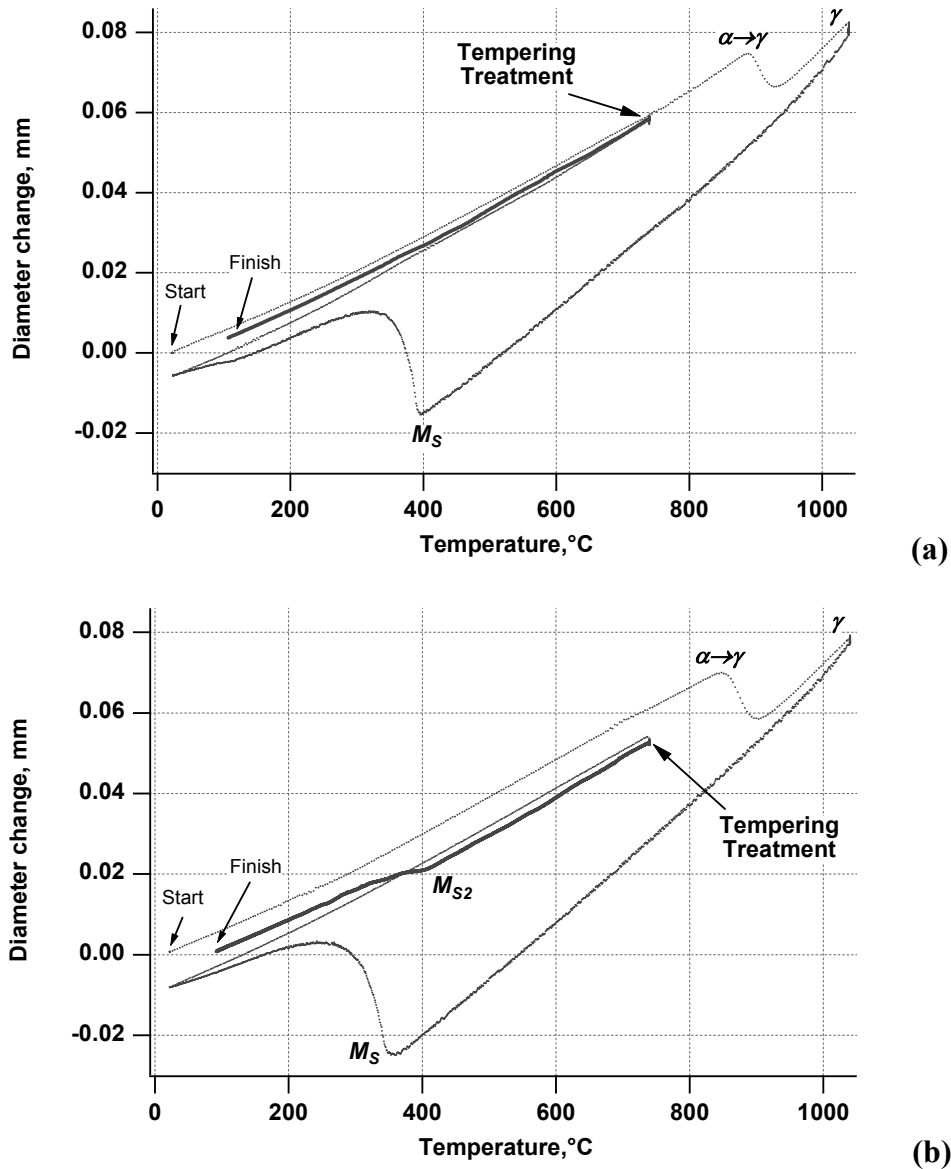


Figure 2. Dilation response of P91 base metal (a), and weld metal (b) during austenitizing, cooling to room temperature and tempering treatments.

sufficiently high that further transformation after tempering is undetectable by this experimental technique.

The weld deposit behavior is not consistent with the M_F prediction of about 150-170°C. According to the M_F relationship, the martensite transformation in the weld deposit should have been completed upon cooling to room temperature. However, the dilation results shown in Fig. 2(b) indicate that the microstructure contained austenite after the tempering cycle. Some or all of the austenite retained after tempering transformed to martensite at around 400°C during the final cooling stage. This means that the weld deposit contained some untempered martensite at the completion of the heat treating cycle.

X-ray Diffraction Measurements

The variations of diffracted intensities in the base metal and weld metal during the later stage of initial cooling to room temperature, the tempering treatment, and final cooling to room temperature are shown in Fig. 3. Technical difficulties precluded accurate monitoring of incident X-ray flux, so the diffraction patterns were normalized to a constant total signal. Even so, vertical bands are apparent where this normalization was not valid. Gaps in the data

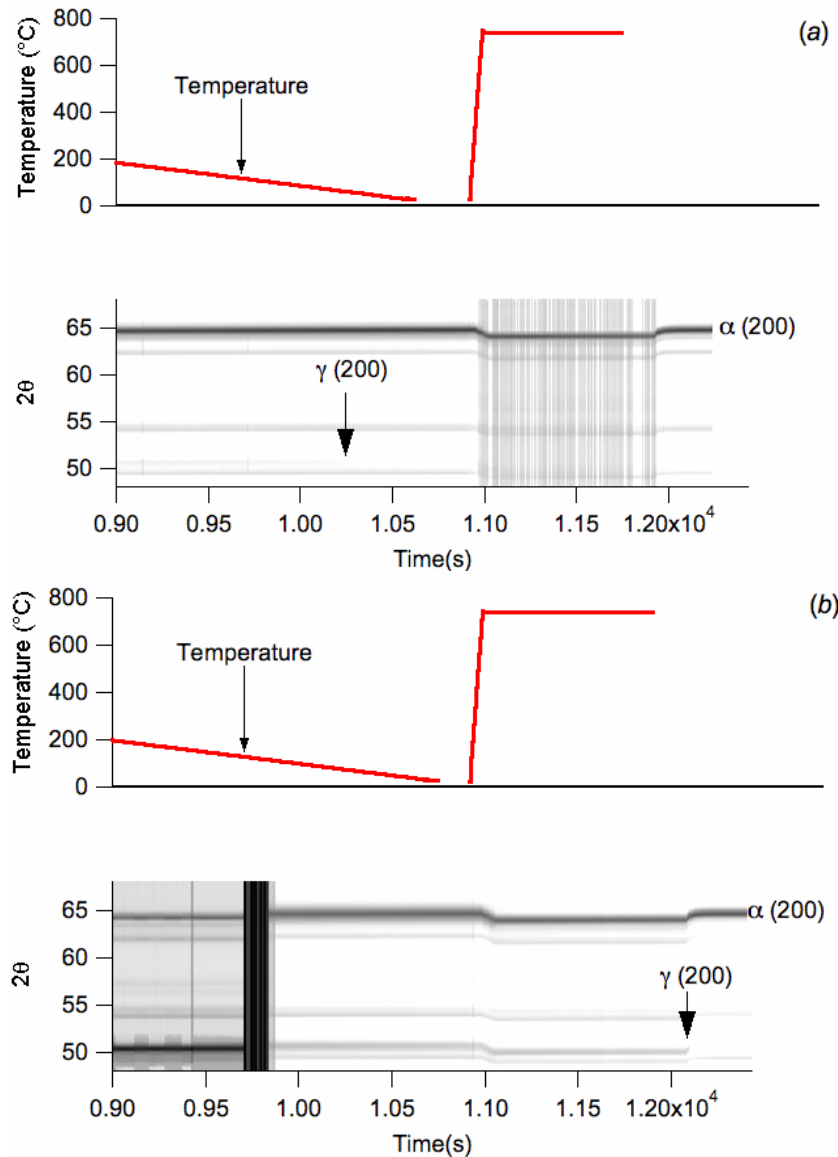


Figure 3. Variations of temperature and diffracted intensities with time for: (a) base metal, and (b) weld metal. Times at which austenite γ (200) peaks disappear are arrowed. Unmarked intensity lines originated from surface oxides.

correspond to times when x-rays were not available. The results from the base metal, Fig. 3(a), show that the austenite (200) diffraction peaks disappeared while cooling from the austenitizing temperature. This indicates there was complete transformation of austenite to martensite, in agreement with dilatometric measurements. In contrast, the results from the weld metal, Fig. 3(b) show that the austenite (200) diffraction peaks are present even after initial cooling to room temperature. Area fraction analysis of the ferrite (200) and austenite (200) diffraction peaks indicated an approximate residual austenite percentage of about 9% at room temperature prior to the tempering treatment. During the tempering treatment, there was an initial increase in austenite diffracted intensities followed by a gradual decrease during the isothermal hold at 740°C. This variation in intensity indicated that the amount of austenite increased initially to about 12% and then decreased back to about 9%. In addition, the peak position of austenite (200) increased to higher 2θ values indicating that the austenite lattice parameter decreased during the tempering treatment. Redistribution of both substitutional solutes and interstitial solutes could reduce the austenite lattice parameter, but redistribution of interstitial carbon is much more likely. On cooling from the tempering temperature, the residual austenite in the

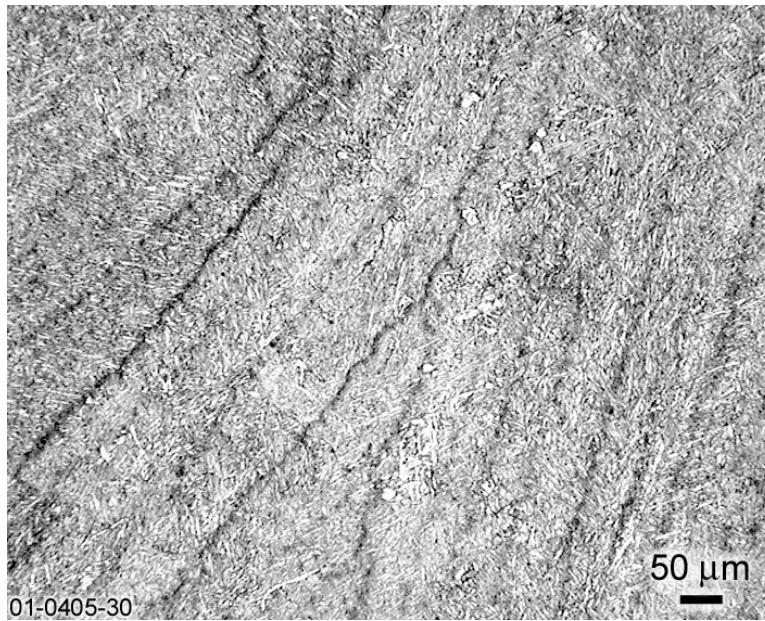


Figure 4. Optical micrograph showing the microsegregation pattern superimposed on the tempered martensite structure of the P91 weld metal.

weld metal transformed to martensite, and, at room temperature, there was no significant austenite (200) peak intensity.

The x-ray diffraction results are consistent with the conclusions drawn from the dilatometric measurements. In summary, the weld metal contained a small amount of residual, untransformed austenite after cooling to room temperature from the austenitizing treatment. On heating to the 740°C tempering treatment, the amount of retained austenite appeared to increase slightly. With holding time at 740°C, the amount of austenite decreased to near its original level, and its lattice parameter also decreased. This retained austenite transformed to martensite on cooling from the tempering treatment.

Microsegregation Analysis

The microsegregation in the weld metal is illustrated by Fig. 4. This microsegregation pattern has a spacing of 50-100 μm which is consistent with the dendrite arm spacing expected in submerged arc welds of steels [11]. The segregation behavior of an alloy having the weld metal composition was analyzed using computational thermodynamics (ThermoCalc™). The predicted variations of C, Cr, Mn, and Ni with fraction solid were calculated assuming the nonequilibrium solidification (Scheil) conditions of local equilibrium at the liquid-solid interface, no solid diffusion, and complete diffusion in the liquid during solidification [12,13]. The results, shown in Fig. 5(a) for C and Cr and in Fig. 5(b) for Mn and Ni, represent the approximate elemental microsegregation gradients in the solidified microstructure at its solidus. All of these important alloying elements preferentially partition to the liquid during solidification. According to these predictions, enrichment of the liquid with the combination of C, Cr, Ni, and Mn actually produces a shift in solidification mode from primary ferrite to primary austenite at a solid fraction greater than about 0.97. This event accounts for the step discontinuities shown in Figs. 5. The thermodynamic predictions also indicate that about 1 wt% of M(C,N) phase forms in the very last stage of the solidification process.

Influence of Microsegregation on Austenite Transformation Behavior

The experimental data confirm that the austenite transformation behavior of the wrought base metal alloy is different than that of the weld metal alloy. Unfortunately, the analyses conducted thus far do not establish the exact reasons for the difference. However, there is little doubt that microsegregation in the weld metal must influence its overall transformation characteristics.

Even though there is only indirect evidence of it as shown by Fig. 4, there is no question that microsegregation occurred in this weld metal. Weld metal may experience repeated high temperature excursions as successive weld beads are deposited. Additionally, weldments may be subjected to extended post weld heat treatments at low temperatures, as in the present case. However, homogenization, particularly of substitutional alloying elements, will typically require much longer high temperature heat treatments than weld deposits will experience during welding and low-temperature post weld heat treatments [14,15]. Consequently, microsegregation will be persistent in this type of weld metal. Because the weld metal composition will not be homogeneous, its transformation behavior will not be uniform throughout its microstructure, but it will depend on local chemical composition.

Microsegregation will have two important effects in P91 weld deposits. Interdendritic regions that are enriched in C, Cr, Ni, and Mn will have lower M_S 's than the nominal composition would imply. These regions will also have lower M_F 's. One manifestation of these characteristics in P91 weld deposits would be wider ranges of martensite transformation temperatures compared to wrought materials.

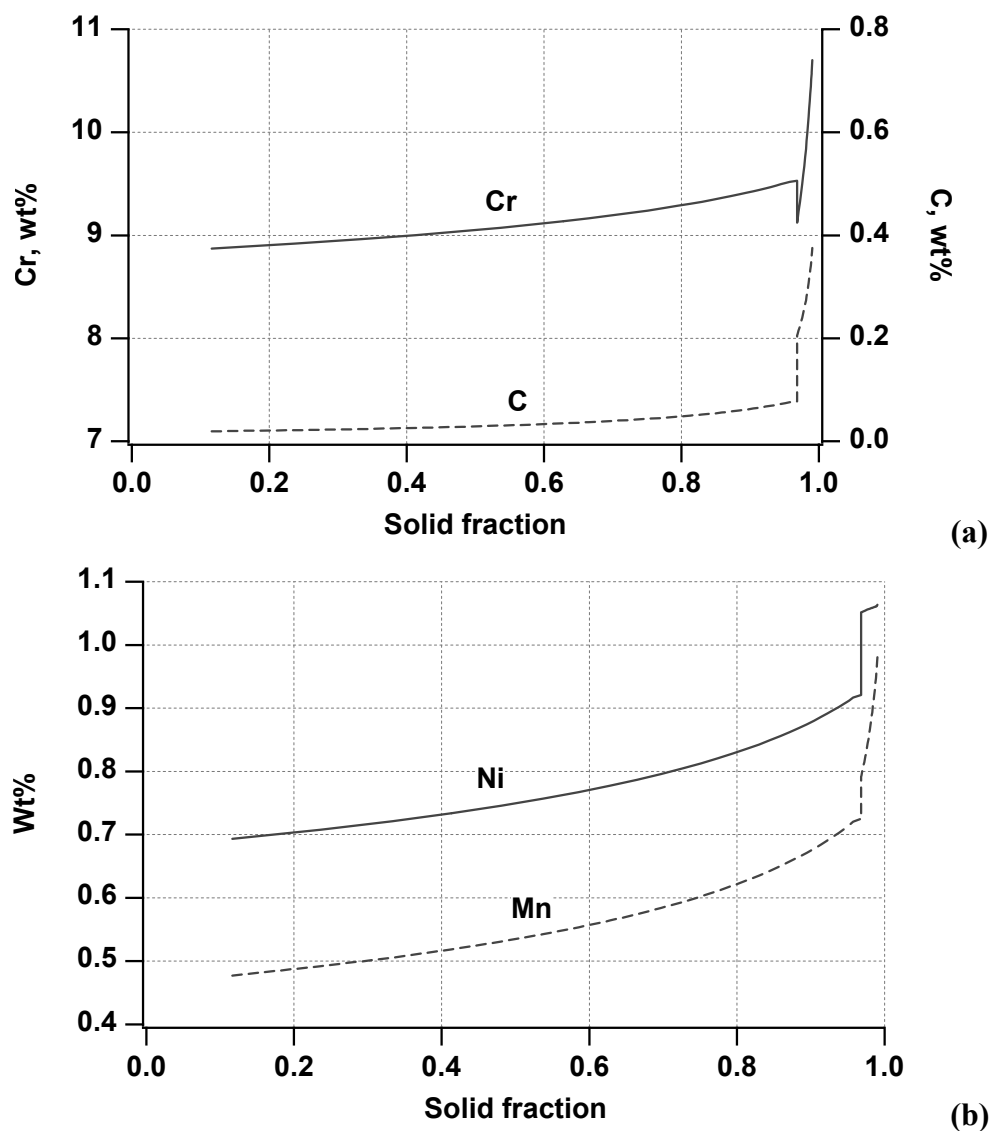


Figure 5. Calculated variations of (a), C and Cr, and (b), Mn and Ni concentrations with solid fraction during solidification of weld metal alloy assuming Scheil-Gulliver model.

Microsegregation will also influence other transformation temperatures. In P91 alloys, Mn and Ni have relatively strong effects on the low temperature ferrite-to-austenite transformation temperature, $A1$ [16]. For instance, equilibrium calculations indicate that the $A1$ temperatures for austenite of the composition range predicted to form during solidification of the weld metal are in the range of 704-717°C. Of course, these predictions ignore the effects of solid-state diffusion during solidification and cooling, welding, and post weld heat treatments. The effects of carbide precipitation subsequent to solidification are also ignored. However, it seems likely that the 740°C tempering temperature would have exceeded the $A1$ of interdendritic regions of elevated Mn and Ni concentrations. The dilatometric and x-ray diffraction data showing stable austenite at 740°C are consistent with this prediction.

The behavior of the retained austenite during the tempering treatment may also be rationalized by arguments based on microsegregation effects. During the tempering treatment, the retained austenite may grow slightly as the x-ray data indicate to satisfy local equilibrium or paraequilibrium conditions [17,18]. However, a more important observation is that the austenite lattice parameter decreases during tempering. A decrease in lattice parameter indicates that alloying elements are being removed from solution in the austenite. This could be the result of the growth of $M(C,N)$ particles that occur interdendritically, or by the nucleation and growth of $M_{23}C_6$ precipitates. Either of these events are likely at the tempering temperature, and they would decrease the C concentration of the austenite and thereby its lattice parameter. Reducing the C concentration of the retained austenite would also increase its M_S . This behavior is also consistent with the experimental measurements.

Summary and Conclusions

Dilatometric and x-ray diffraction measurements during controlled thermal cycles were used to follow austenite decomposition in a P91 base metal and in a weld deposit that was previously post weld heat treated at 774°C (1425°F) for 8 h. The measurements showed that the transformation behaviors were substantially different. The austenite-to-martensite transformation was completed in the base metal during initial cooling from the 1040°C austenitizing temperature. The M_S measured in the base metal, 393°C, agreed closely with that predicted from expressions based on experimental data, 383°C.

In contrast, the austenite-to-martensite transformation was only completed in the weld metal after a 740°C tempering treatment. The dilatometric measurements showed that a secondary martensite reaction occurred in the weld metal during cooling from the 740°C. This secondary martensite reaction occurred at a higher temperature, $M_{S2} \approx 400^\circ\text{C}$, than the primary martensite transformation, $M_S \approx 350^\circ\text{C}$. X-ray diffraction measurements conducted during nominally identical thermal treatments confirmed that austenite was retained in the weld metal during cooling from 1040°C and during the tempering treatment, and that it transformed to martensite in the final cooling stage. The x-ray diffraction measurements also indicated that the lattice parameter of the austenite retained during tempering decreased. A decrease of lattice parameter is consistent with decreased solute content in the retained austenite and with a secondary M_S that is different than the primary M_S .

The stability of austenite in the weld metal during initial cooling from an austenitizing treatment and during tempering, and its transformation behavior to martensite were attributed to the effects of microsegregation.

Acknowledgement

This research, done at Oak Ridge National Laboratory, was sponsored by the Office of Fossil Energy, Advanced Research Materials Program, (DOE/FE AA 15 10 10 0) U.S. Department of Energy under Contract DE-AC05-00OR22725 with UT-Battelle, LLC. The assistance with metallographic specimen etching provided by George VanderVoort of Buehler Ltd. was invaluable. The assistance of Gene Ice and Paul Zschack with the diffraction experiments, and review of the manuscript by Marimuthu Muruganath and Phil Maziasz was appreciated.

The UNICAT facility at the Advanced Photon Source (APS) is supported by the Univ of Illinois at Urbana-Champaign, Materials Research Laboratory (U.S. DOE, the State of Illinois-IBHE-HECA, and the National Science Foundation), the Oak Ridge National Laboratory, the National Institute of Standards and Technology (U.S. Department of Commerce) and UOP LLC. The APS is supported by the U.S. DOE, Basic Energy Sciences, Office of Science under contract No. W-31-109-ENG-38.

References

1. F. V. Ellis, J. F. Henry, and B. W. Roberts, "Welding, Fabrication, and Service Experience with Modified 9Cr-1Mo Steel," pp. 55-63 in *New Alloys for Pressure Vessels and Piping*, PVP Volume 201, American Society of Mechanical Engineers, NY, 1990
2. T. Wada, *The Continuous Cooling Transformation Diagram and Tempering Response of 9Cr-1Mo-V-Nb Steels*, J-4672, Climax Molybdenum Company of Michigan, Ann Arbor, MI, 1981
3. V. K. Sikka, C. T. Ward, and K. C. Thomas, "Modified 9Cr-1Mo Steel – An Improved Alloy for Steam Generator Application," pp. 65-84 in *Ferritic Steels for High-Temperature Applications*, edited by A. K. Khare, American Society for Metals, Metals Park, OH, 1983
4. G. C. Bodine, C. Chakravarti, C. M. Owens, B. W. Roberts, D. M. Vandergriff, and C. T. Ward, *A Program for the Development of Advanced Ferritic Alloys for LMFBR Structural Application*, ORNL/Sub-4291/1, TR-MCD-015, Oak Ridge National Laboratory, 1977
5. W. B. Jones, C. R. Hills, and D. H. Polonis, "Microstructural Evolution of Modified 9Cr-1Mo Steel, *Metallurgical Transactions A*, vol. 22A, pp. 1049-1058, (1991).
6. R. H. Haigh, M. Strangwood, and D. J. Widgery, "Carbonitride Population Development in 9Cr-1Mo Weldments," pp. 253-258 in *Trends in Welding Research, Proceedings of the 4th International Conference*, edited by H. B. Smartt, J. A. Johnson, and S. A. David, ASM International, Metals Park, OH, 1996.
7. G. T. Eldis, "A Critical Review of Data Sources for Isothermal Transformation and Continuous Cooling Transformation Diagrams," pp. 126-157 in *Hardenability Concepts with Applications to Steels*, edited by D. V. Doane and J. S. Kirkaldy, TMS, Warrendale, Pennsylvania, 1978.
8. G. A. Knorovsky, C. V. Robino, R. C. Dykhuizen, and D. O. MacCallum, "Dilatometry in the Gleeble: What Did You Really Measure?," pp. 101-106 in *Trends in Welding Research, Proceedings of the 5th International Conference*, edited by J. M. Vitek, S. A. David, J. A. Johnson, H. B. Smartt, and T. DebRoy, ASM International, Metals Park, OH, 1999.
9. L Béres, W. Irmer, and A. Balogh, "Inconsistency of classification of creep resistant steels in European standard EN 288-3," *Science and Technology of Welding and Joining*, vol. 2, pp. 236-238, (1997)

10. L Béres, A. Balogh, and W. Irmer, "Welding of Martensitic Creep-Resistant Steels," *Welding Journal*, vol. 80(8), pp. 191-s-195-s, (2001)
11. S. A. David and J. M. Vitek, "Correlation between solidification parameters and weld microstructures," *International Materials Reviews*, vol. 35(5), pp. 213-245, (1989)
12. B. Sundman, B. Jansson, and J. O. Andersson, "The thermo-calc databank system," *Calphad*, 1985, **9**, 1-153
13. N. Saunders and A. P. Miodownik, *Calphad (Calculation of Phase Diagrams): A Comprehensive Guide*, Pergamon Materials Series, Volume 1, Elsevier Science Inc., New York, 1998
14. *Steels: Microstructure and Properties*, Second edition, R. W. K. Honeycombe and H. K. D. H. Bhadeshia, Chapter 1, Edward Arnold, London, UK, 1995
15. *Fundamentals of Solidification*, Fourth revised edition, W. Kurz and D. J. Fisher, Appendix 13, Trans Tech Publications Ltd, Switzerland, 1998.
16. M. L. Santella, R. W. Swindeman, R. W. Reed, and J. M. Tanzosh, "Martensite formation in 9 Cr-1 Mo steel weld metal and its effect on creep behavior," in EPRI Conference on 9 Cr Materials Fabrication and Joining Technologies, EPRI, Palo Alto, California, 2001
17. J. D. Robson and H. K. D. H. Bhadeshia, "Modelling the Development of Microstructure in Power Plant Steels," pp. 179-207, in *Microstructural Development and Stability of High Chromium Ferritic Power Plant Steels*, edited by A. Strang and D. J. Gooch, Institute of Materials, London, UK, 1997
18. M. Hillert, "Nature of local equilibrium at the interface in the growth of ferrite from alloyed austenite," *Scripta Materialia*, 2002, **46**, 447-453

This manuscript has been authored by a contractor of the U.S. Government under contract DE-AC05-00OR22725. Accordingly, the U.S. Government retains a nonexclusive, royalty-free license to publish or reproduce the published form of this contribution, or allow others to do so for U.S. Government purposes.